Very Small Size k_a Band 6 Bit DMTL Phase Shifter Based on Combination of Capacitor and Resonator Type Methods

Erfan Cheshmeh, Saeid Afrang
Electrical Engineering Dept., Urmia University, Urmia, Iran
e.cheshmeh@gmail.com, s.afrang@urmia.ac.ir
Corresponding author: s.afrang@urmia.ac.ir

Abstract- **Design and simulation of a very small size 6-bit DMTL phase shifter is presented. The idea is based on using both capacitor and resonator type methods simultaneously in a phase shifter. The capacitor section creates less significant bits. The bits in this section start from the least significant bit, with 5.625-degree steps. The resonator section creates the bits with 90-degree steps. CPW transmission line is used as an impedance matching between two type phase shifters. The structure is calculated and simulated at the Ka-band using MATLAB and HFSS softwares, respectively. The proposed method decreases the number of cells, considerably. As a result, the size and loss is decreased. The design can be easily scaled to other frequencies for satellite and radar systems.**

Index Terms- Phase shifter, Small Size, Capacitor, Resonator, K_a Band.

I. INTRODUCTION

RF MEMS devices, in general, outperform conventional semiconductor-based modules. The advantages offered by RF MEMS technology can be briefly summarized as follows[1-3]: low-loss performance at high-frequency ranges, enhanced isolation, wide-band performance, minimal DC power consumption (when the switch is in the OFF state), high linearity, high power-handling capacity, low parasitic effects. The phase shifter is an important device in communication systems. It should be designed in such a way that it reduces electromagnetic interference and size should be small to consume less power. In order to overcome the defects of conventional electronics beam steering, Phase shifters are widely used in phase array antennas. To overcome the huge size and the losses that conventional phase shifters exhibit, RF MEMS phase shifters are used in phased-array radar applications. RF MEMS-based switches provide low-loss performance in phase shifters over a wide range of frequencies. MEMS-based Phase Shifters can either be analog or digital. Analog phase

shifters using coplanar waveguide (CPW) lines with distributed micro-electro-mechanical system (MEMS) bridges demonstrated broad-band characteristics with the low loss [4]. However, since there was a limit on the control range of the bridge height before the bridge snaps, the analog phase shifter showed relatively a small phase shift. This problem was solved by operating the MEMS bridges in the digital mode [5-9].

All kinds of the MEMS phase shifters have a large size compared to solid state phase shifters. It is essential that the area of RF MEMS phase shifter be reduced. The advantages of reduced size are many: easier in hermetic packaging, much higher part count per wafer, and much lower cost and loss. Initially, the primary distributed MEMS transmission line (DMTL) phase shifters were large in size [4-5]. To decrease the size, Afrang et al. [9] presented a new concept of DMTL phase shifter using both capacitors and inductors. Based on their proposed structure and around the resonance frequency it is possible to achieve a large phase shift together with reasonable return loss. Recently, Lin et al. [10] reported on a miniature DMTL phase shifter using both tunable capacitors and inductors. Based on their proposed structure when increasing capacitance of the cell in the actuated condition to obtain a large phase shift, the value of the tunable inductor is also increased, keeping Zdown matched to the port impedance while further increasing the phase shift.

This work presents a very small size of MEMS phase shifter using both capacitor and resonator type methods simultaneously in a phase shifter. In the proposed phase shifter the capacitor type section creates less significant bits and the resonator type phase shifter section creates more significant bits. As a result, the size and loss are decreased.

II.   DESIGN CONSIDERATIONS

Fig. 1 shows the schematic diagram of the proposed structure. It is the modified structure of the DMTL phase shifter proposed by Afrang [7] and Afrang et al.[8]. As shown in Fig. 1a, the structure consists of three sections: impedance matching, capacitor and resonator type phase shifter sections. Fig. 1b and 1c show the least significant bit in the capacitor and resonator section, respectively.

The least significant bit in the capacitor type phase shifter section consists of a coplanar waveguide (CPW) line, a MEMS capacitive switches together with two additional electrodes near the centerline under the bridge, and two static MAM capacitors connected to the ends of the bridge. The height of the additional electrodes is more than the lower electrode in the middle of the switch. The initial gap between the bridge with a center line and additional electrodes is G0 and G1 respectively. With the aid of additional electrodes, it is possible to have two phase states in a unit cell. When the voltage is applied between the additional electrodes and MEMS bridge, the bridge touches the electrodes. In this condition, the phase of the unit cell is tuned to changes 5.625°. If the voltage is applied between the bridge and the lower electrode in the middle of the bridge, the bridge touches the middle electrode. Again in this condition, the phase of the unit cell is tuned to changes 11.25°.
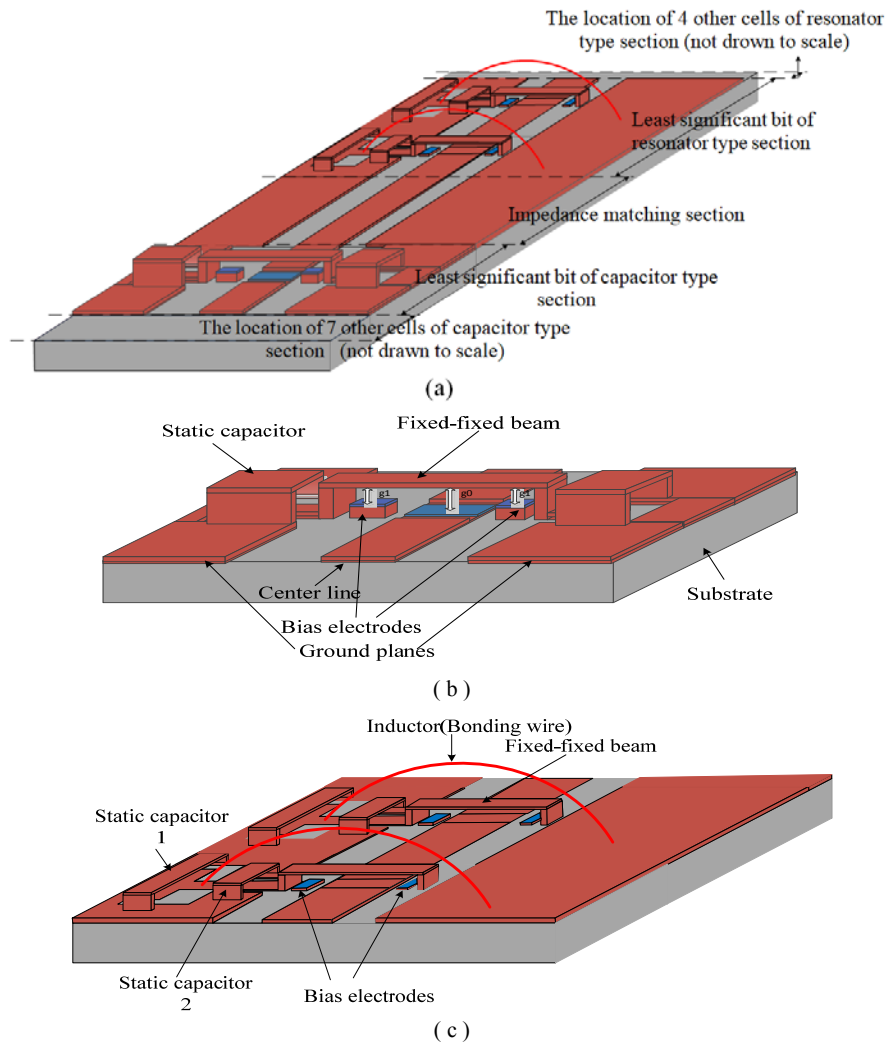
The location of 4 other cells of resonator type section (not drown to scale)

Least significant bit of resonator type section

Impedance matching section

Least significant bit of capacitor type section

The location of 7 other cells of capacitor type section (not drawn to scale)

(a)

Static capacitor Fixed-fixed beam

g1 g0 g1

Center line Substrate

Bias electrodes
Ground planes

(b)

Inductor(Bonding wire)
Fixed-fixed beam

Static capacitor 1

Static capacitor 2 Bias electrodes

(c)

Fig. 1. (a) Schematic diagram of the proposed phase shifter, (b) least significant bit in the capacitor section, (c) least significant bit in the resonator section

The least significant bit in the resonator type phase shifter section consists of two cells. Each cell is composed of a coplanar waveguide line, a static MAM capacitor, a bonding wire as an inductor, a fixed-fixed beam and a bias electrodes. The fixed-fixed beam together with bias electrodes makes a MEMS switch. The bonding wire is in parallel with the static capacitor. One end of the static capacitor and the bonding wire is grounded and another end of them is connected to the beam anchor. In the initial condition and with no applied voltage, the bridges in least significant bit are in the upstate position. There is an AC capacitor between the bridges and the center line in the upstate position. When the switches are in the downstate position, the bridges are directly connected to the parallel LC circuit.

Fig. 2 shows the equivalent circuit of Fig. 1b. In this circuit, the distributed parameters for the transmission line have been used where L_t, C_t, and R_t are per unit length inductance, capacitance and
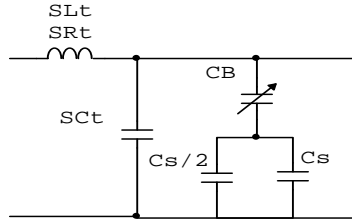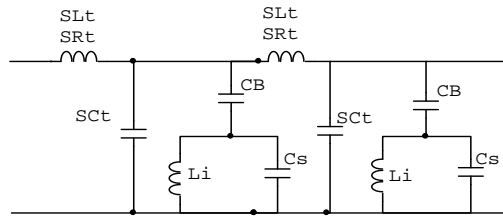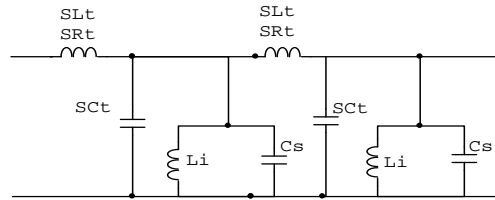
Fig. 2. Equivalent circuit of Fig. 1b

(a)

(b)

Fig. 3. Equivalent circuit of figure 1c in the (a) up and (b)
down state position

resistance of the transmission line respectively, and "S" is the periodic separation between MEMS switches. As represented in the equivalent circuit, the design is composed of an unloaded line loaded with MEMS switch in series with lumped element capacitors (Cs/2).

Fig. 3a and 3b show the equivalent circuit of Fig. 1c in the up and down state position, respectively. In these circuits, the distributed parameters for the transmission line have been used where Lt, Ct, and Rt are per unit length inductance, capacitance and resistance of the transmission line respectively, and ''S'' is the periodic separation between MEMS switches.

Fig. 4a and 4b show the equivalent circuit of the whole proposed phase shifter (Fig. 1a) in the up and down state position, respectively.
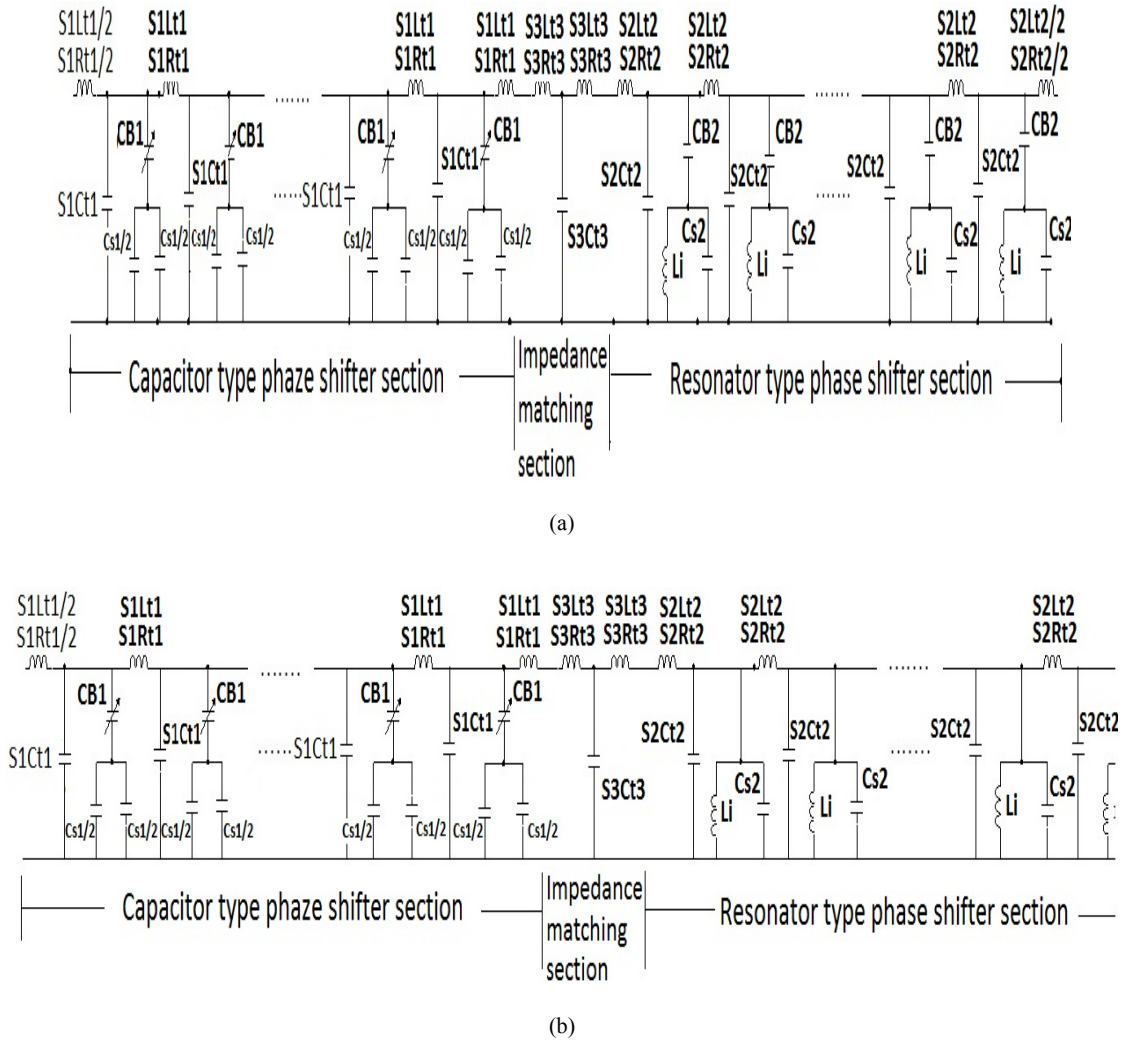
(a)

(b)

Fig. 4. Equivalent circuit of the whole structure (Fig. 1a) of the proposed phase shifter in the (a) up and
(b) down state position

A. *Derivation of Scattering Parameters*

The distributed line phase shifter can be conveniently analyzed using the ABCD matrices. To derive
S11 in terms of ABCD-parameters, the equivalent circuit in Fig. 5 is used.

In this circuit, Zo2 is a matched transmission line. Zo1 is the characteristic impedance of the lossy
transmission line. The length of the lossy transmission line determines the periodic separation. The
structure is placed after this line. The term (GL + jBL) is the shunt load. S_{11} in terms of ABCD-
parameters of the structure and matched transmission line Z_{O2} is as following (Wolff & Kaul 1988):

$$S_{11} = \frac{A + BY_{O2} - C.Z_{O2} - D}{A + BY_{O2} + C.Z_{O2} + D}$$

(1)

The ABCD matrix of the lossy transmission line is given by:
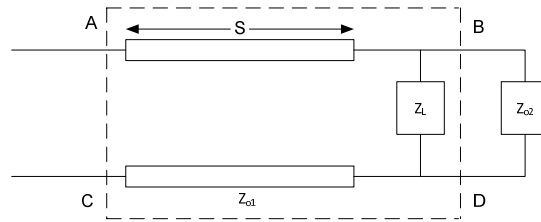
Fig. 5. Circuit for derivation of S_{11}

$$\begin{bmatrix} A_1 & B_1 \\ C_1 & D_1 \end{bmatrix} = \begin{bmatrix} \cosh(\gamma.s) & Z_{o1}.\sinh(\gamma.s) \\ Y_{o1}.\sinh(\gamma.s) & \cosh(\gamma.s) \end{bmatrix}$$

(2)

$$\gamma = \alpha + j\beta$$

where, γ, α and β are the complex propagation constant, attenuation and the phase constant of the transmission line respectively. α and β are as following:

$$\alpha = \frac{sR_t}{2Z_o}$$

$$\beta = \frac{\omega}{v_p}$$

(3)

where, R_t is the resistance per unit length given by:

$$R_t = \frac{\rho}{\delta.w}$$

(4)

Where ρ $(\Omega - cm)$ is the metal resistivity, w is the width of the center line, and δ is the skin depth given by:

$$\delta = \sqrt{\frac{\rho}{\pi \mu f}}$$

(5)

$$v_p = \frac{1}{\sqrt{(sL_t)(sC_t)}}$$

(6)

The per unit length inductance and capacitance of a transmission line are determined to be:

$$L_t = \frac{\sqrt{\varepsilon_{eff}}Z_O}{C}$$

$$C_t = \frac{\sqrt{\varepsilon_{eff}}}{Z_0 C}$$

(7)

where, ε_{eff} is the effective dielectric constant of the unloaded line. The effective dielectric constant is approximated by assuming half of the fields are present in the air above the metallization and the other half is in the substrate.
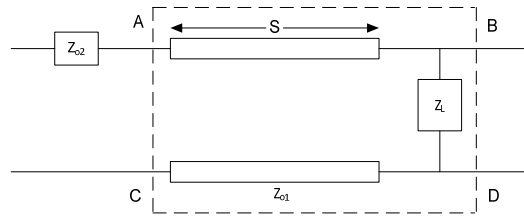
Fig. 6. Circuit for derivation of S_{21}

$$\varepsilon_{eff} = \frac{\varepsilon_r + 1}{2} \tag{8}$$

The ABCD matrix of the shunt load is given by:

$$\begin{bmatrix} A_2 & B_2 \\ C_2 & D_2 \end{bmatrix} = \begin{bmatrix} 1 & 0 \\ Y_L & 1 \end{bmatrix} \tag{9}$$

The overall ABCD matrix of the structure is obtained as:

$$\begin{bmatrix} A & B \\ C & D \end{bmatrix} = \begin{bmatrix} cosh(\gamma.s) & Z_{o1}.sinh(\gamma.s) \\ Y_{o1}.sinh(\gamma.s) & cosh(\gamma.s) \end{bmatrix} * \begin{bmatrix} 1 & 0 \\ Y_L & 1 \end{bmatrix} \tag{10}$$

To derive S_{21} in terms of ABCD-parameters, the equivalent circuit in Fig. 6 is used. The source impedance Z_{O2} must be included in the calculation to separate incident and reflected waves. S_{21} in terms of ABCD-parameters is as following:

$$S_{11} = \frac{2}{A + B.Y_{02} + C.Z_{02} + D} \tag{11}$$

Finally, the phase angle of S_{21} determines the phase of the structure in the up or down state position. The phase difference between up and down state position at a given frequency determines the phase shift of the structure.

B. Design of Capacitor Type Section of the Phase Shifter

In the capacitor type MEMS phase shifters the bridge capacitor serves to lower the impedance in the up and down state position. Therefore the unloaded impedance of the transmission line must be greater than the highest load impedance. Consider the DMTL is placed within a 50 Ω system. The desired DMTL loaded impedances in terms of the maximum desired reflection coefficient is obtained by:

$$Z_t = 50 \sqrt{\frac{1 \pm \Gamma_{in}}{1 \mp \Gamma_{in}}} \tag{12}$$

where, Γ_{in} is the input return loss of the structure. The solution to this equation for maximum return loss of -15dB gives Z_{lu}=59.8 and Z_{ld}=41.8. These impedances are the optimal load impedance at the design frequency to maximize the phase shift while keeping the reflected power loss at the input of the DMTL to a design specified minimum. These impedances represent the maximum (Z_{lu}) and minimum (Z_{ld}) impedances of the DMTL in the up and down states of the MEMS bridge, respectively. The capacitor type phase shifter section creates the phase shifts with smaller significant bits including 5.625°, 11.25°, 22.5° and 45°. The following expressions, combined with the Bragg frequency are solved to develop closed-form design equations for two-phase states in a unit cell of the DMTL phase shifter:

$$s = \frac{Z_{ld2}C}{\pi f_B Z_o \sqrt{\varepsilon_{r,eff}}} \ \ \text{meters} \tag{13}$$

$$C_{lu} = \frac{(Z_0^2 - Z_{lu}^2)Z_{ld2}}{Z_0^2 Z_{lu}^2 \pi f_B} \ \ \text{farads} \tag{14}$$

$$C_{ld1} = \frac{(Z_0^2 - Z_{lu}^2)Z_{ld2}}{Z_0^2 Z_{ld1}^2 \pi f_B} \ \ \text{farads} \tag{15}$$

$$C_{ld2} = \frac{(Z_0^2 - Z_{ld2}^2)}{Z_0^2 Z_{ld2} \pi f_B} \ \ \text{farads} \tag{16}$$

$$\Delta\varphi_1 = \frac{360° s\omega Z_o \sqrt{\varepsilon_{r,eff}}}{C}\left(\frac{1}{Z_{lu}} - \frac{1}{Z_{ld1}}\right) \ \ \frac{\text{degree}}{\text{section}} \tag{17}$$

$$\Delta\varphi_2 = \frac{360° s\omega Z_o \sqrt{\varepsilon_{r,eff}}}{C}\left(\frac{1}{Z_{lu}} - \frac{1}{Z_{ld2}}\right) \ \ \frac{\text{degree}}{\text{section}} \tag{18}$$

In this study, the Bragg frequency is selected to be approximately 2.4 times the design frequency at 30 GHz. The CPW line dimensions are 100/100/100 μm (Z_o = 96Ω, ε_r = 3.75) with the corresponding separation of 300 μm at 38 GHz. On the other hand, the maximum and minimum impedance of the DMTL in the up and down states of the MEMS bridge (Z_{lu} = 60, Z_{ld2} = 42) with Z_{ld1} = 49 satisfy the phase states of 11.25° and 5.625° respectively at 38 GHz. Finally, the corresponding load capacitances in the up, first step and second step of downstate position are C_{lu}=24 fF, C_{ld1} = 33 fF, and C_{ld2} = 66 fF respectively.
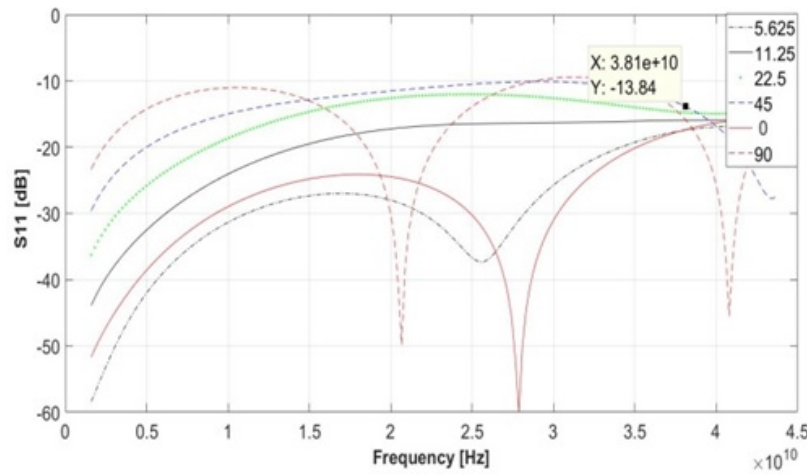
To draw return loss and phase shift versus frequency diagrams the equation (11) is used. Therefore, it's needed to calculate the overall ABCD matrix of the structure. The admittance (Y_L) of the shunt load in the capacitor type phase shifter section and by neglecting the conductance of them is given by:

$$Y_L = G_L + JB_L \approx J\omega.C_L \tag{19}$$
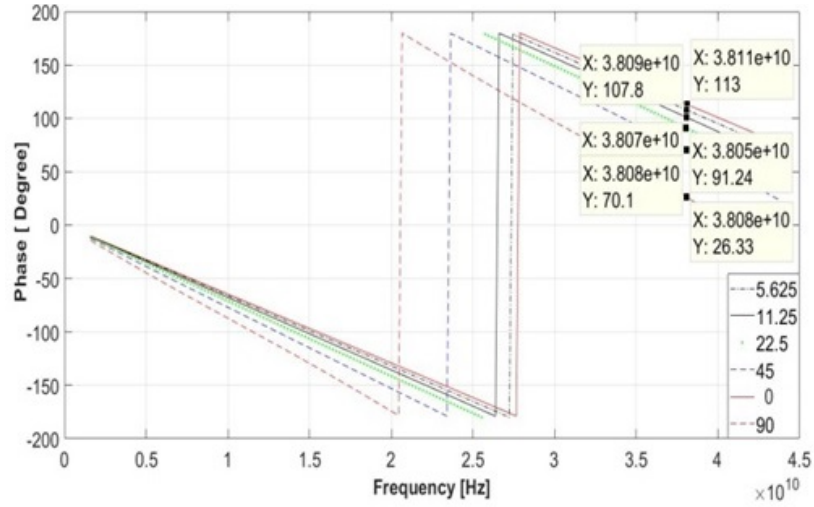
(a)

(b)

Fig. 7. Calculated results of (a) phase and (b) return loss in the capacitor type phase shifter

where,

$$C_L = C_{in} = C_B(up) \parallel C_S$$

$$C_L = C_{ld} = C_B(down) \parallel C_S$$

(20)

If $C_B(up)$=40 fF, $C_B(down) = 1$ pF and C_S =70 fF then $C_{lu} = 24$ fF and $C_{ld} = 66$ fF. In this structure, the metal used is aluminum with the resistivity of $\rho = 2.7$ ($\mu\Omega. cm$). Fig. 7 shows calculated results of return loss and phase shift in the case of capacitor type phase shifter.

C. Design of Resonator Type Section of the Phase Shifter

The resonator type phase shifter section creates the phase shifts with two greater significant bits including 90° and 180°.In the resonator type phase shifter section the resonator serves to move the

structure impedance toward the line impedance. For this reason, the unloaded transmission line impedance is set to 50Ω. The unloaded impedance is selected to meet dimensional layout concerns and to minimize the loss. Higher dielectric constant materials such as silicon and GaAs will produce a bigger phase shift than the one built in quartz. The balancing factor is loss; losses in Si and GaAs are much higher than those in quartz. Therefore, the quartz substrate with the dimension of 15/ 100/15 (Z_o = 50Ω , and ε_r = 3.3) and the aluminum with the resistivity of ρ = 2.7 μΩ.cm for the line is used. The separation, S, between MEMS switches affects the phase shift per section. Increasing the separation, S will increase the phase shift. The penalty paid is increasing the size of the structure. At first S=400 μm is considered. Now, it is possible to calculate the transmission line inductance and capacitance. From Equation (7) and by considering the separation ''s'' the transmission line inductance and capacitance are 98 pH and 39.2 fF, respectively.

The limited space for a unit cell does not allow longer bonding wire. As a result, L=1 nH is considered for the inductor. The exact self-inductance for a straight conductor with a circular cross-section, the magnetic permeability of one and the length with many orders of magnitude greater than radius is [11]

$$L = 0.002l[\ln\left(\frac{2l}{r}\right) - 0.75] \tag{21}$$

To determine the numerical quantity of static and bridge capacitors some issues are considered. From the equivalent circuit in the upstate position, the bridge capacitor is in series with parallel static capacitor and inductor. If the bridge capacitor is very smaller than the static capacitor it dominates the phase of the structure in the upstate position. In the lack of a bridge capacitor, the static capacitor in parallel with an inductor determines the phase of the structure in the down state position. Therefore, to have a large phase difference between the up and down state position large C_s and small C_B are needed. On the other hand, the return loss in the operating frequency should be acceptable. Each cell resonates around resonance frequency in the up and down state position. The return loss is improved around resonance frequencies. If the second cell is connected to the first cell, the second resonance frequencies higher than the first resonance frequencies are formed in the structure. The second resonance frequencies form new areas of operating frequency. Therefore, to have an acceptable return loss and ninety degrees in the least significant bit including two cells using MATLAB software C_B =59 fF and C_s=75 fF is calculated. G_L and B_L for the structure in the upstate position are given by:

$$G_{L(up)} = \frac{-\omega^2 C_B C_{MAM}[1-\omega^2 L_I(C_B+C_{MAM})]+\omega^2 C_B(C_{MAM}+C_B)(1-\omega^2 L_I C_{MAM})}{[1-\omega^2 L_I(C_B+C_{MAM})]^2+\omega^2(C_{MAM}+C_B)^2} \tag{22}$$

$$B_{L(up)} = \frac{\omega C_B(1-\omega^2 L_I C_{MAM})\left(1-\omega^2 L_I(C_B+C_{MAM})+\omega^2 C_B C_{MAM}(C_{MAM}+C_B)\right)}{[1-\omega^2 L_I(C_B+C_{MAM})]^2+\omega^2(C_{MAM}+C_B)^2} \tag{23}$$
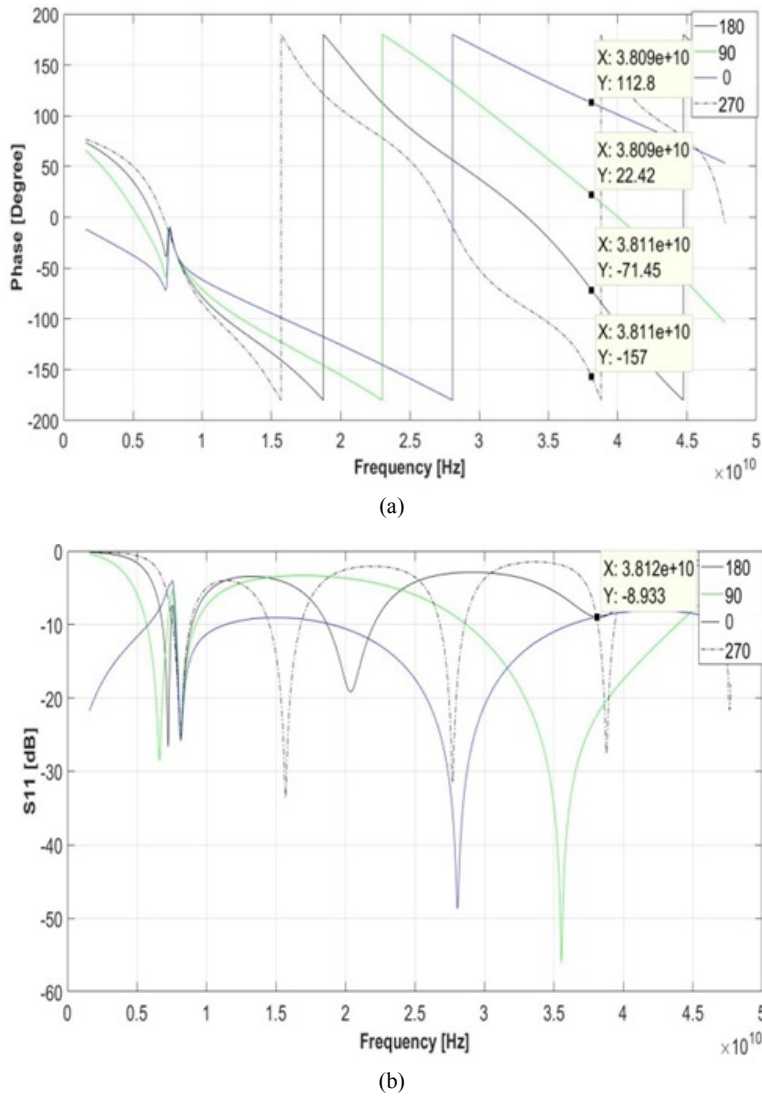
(a)

(b)

Fig. 8. Two bits calculation result of the (a) phase and (b) return loss of the resonator type section, phase shifter.

G_L and B_L for the structure in the down state position are given by:

$$G_{L(down)} = \frac{1}{R_I^2 + \omega^2 L_I^2} \tag{24}$$

$$B_{L(down)} = \frac{\omega R_I^2 C_I - \omega L_I (1 - \omega^2 L_I C_I)}{R_I^2 + \omega^2 L_I^2} \tag{25}$$

Now by considering the exact values of C_S and C_B the phase shift of 90°, 180° and 270° is achieved.

Fig. 8 shows two bits calculation result of the return loss and phase for the resonator type section, phase shifter. As it is seen from Fig. 8, the S11 at 38.1 GHz for all states is smaller than -9 dB.
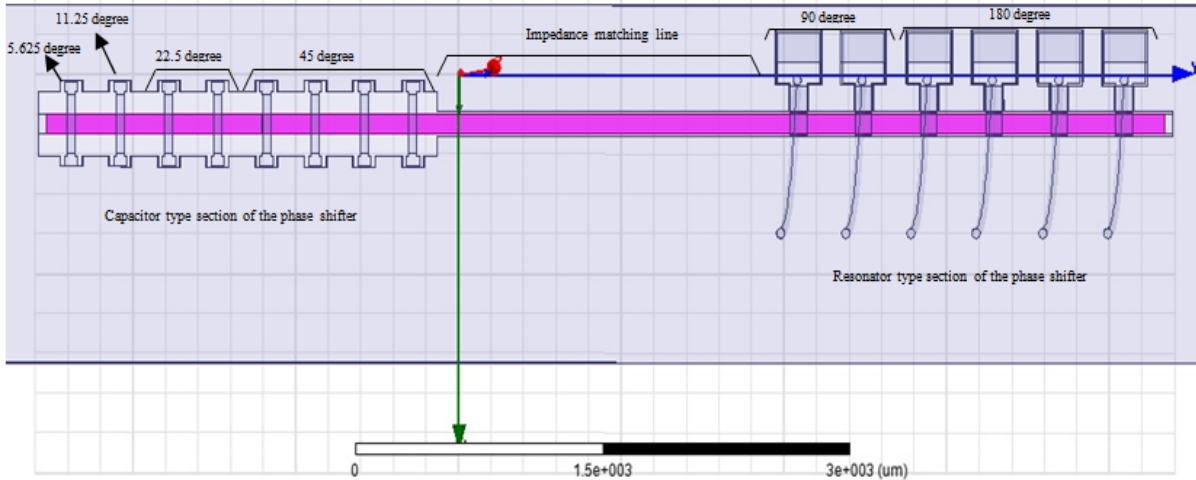
Fig. 9. The schematic of the whole structure

D. Design of the Whole Structure

The impedance of the CPW unloaded line on the resonator type phase shifter section without the MAM cuts in the ground plane is approximately 50Ω. However, fringing capacitance due to the ground plane cuts the t-line impedance to around 40Ω. On the other hand, the impedance of the capacitor type phase shifter section with the MAM cuts and loaded line in the up and down state position is 60Ω and 40Ω respectively. As it is seen, there is impedance mismatching in the contact point between the capacitor and resonator type phase shifter ports. To minimize the return loss due to the mentioned impedance mismatching, the impedance transformer is used. The worst condition occurs when the capacitor type phase shifter section is in the upstate position with 60Ω impedance. Considering 40Ω port impedance in the resonator type phase shifter section, the maximum impedance difference in the contact point is 20Ω. Therefore, the optimum impedance for the impedance matching is 50Ω.

This impedance matching reduces the maximum impedance difference in the contact point from 20Ω to 10Ω. As an impedance transformer and by considering 38.18 GHz working frequency, the impedance transformer length is 2 mm with coplanar dimensions of (15/100/15) micrometer Fig. 9 shows the schematic of the whole structure.

The calculation results of the whole structure are shown in Fig. 10. Fig. 10a shows 90°, (5.625+90)° and (16.875+90)° phases with minimum errors. From the figures, the maximum error phase is around two degrees. Fig. 10b shows the corresponding return loss of the simulated phases. As it is seen, for all phases the return loss is less than -10dB.
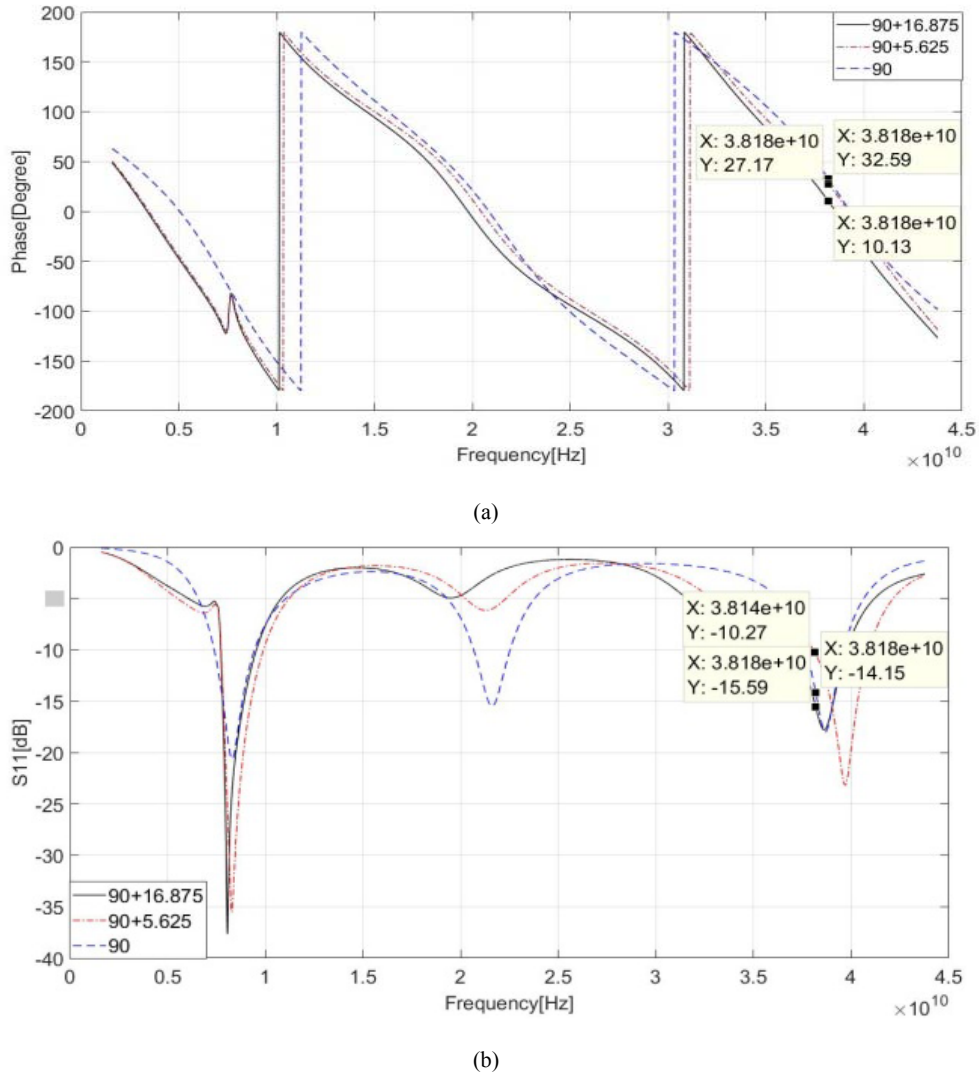
(a)

(b)

Fig. 10. Calculation results of (a) phase and (b) return loss of the whole structure
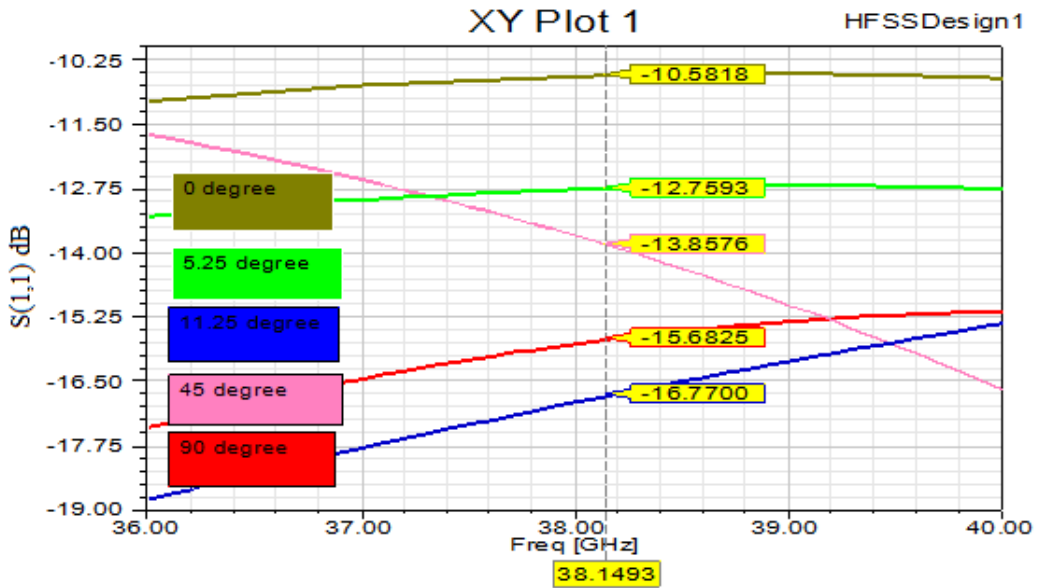
III. SIMULATION RESULTS

To verify, the capacitor section, the resonator section, and the whole structure are simulated using HFSS software.

Fig. 11 shows the simulation results of the capacitor type section of the phase shifter. Fig. 11a shows 5.625°, 11.25°, 45° and 90° phases with minimum errors. From the figures, the maximum error phase is around one degree. Fig. 11b shows the corresponding return loss of the simulated phases. As it is seen, for all phases the return loss is less than -10dB. Fig. 12 shows simulation results of the resonator type section of the phase shifter.

Fig. 12a shows 90°, 180° and 270° phases with minimum errors. From the figures, the maximum error phase is around two degrees. Fig. 12b shows the corresponding return loss of the simulated phases. As
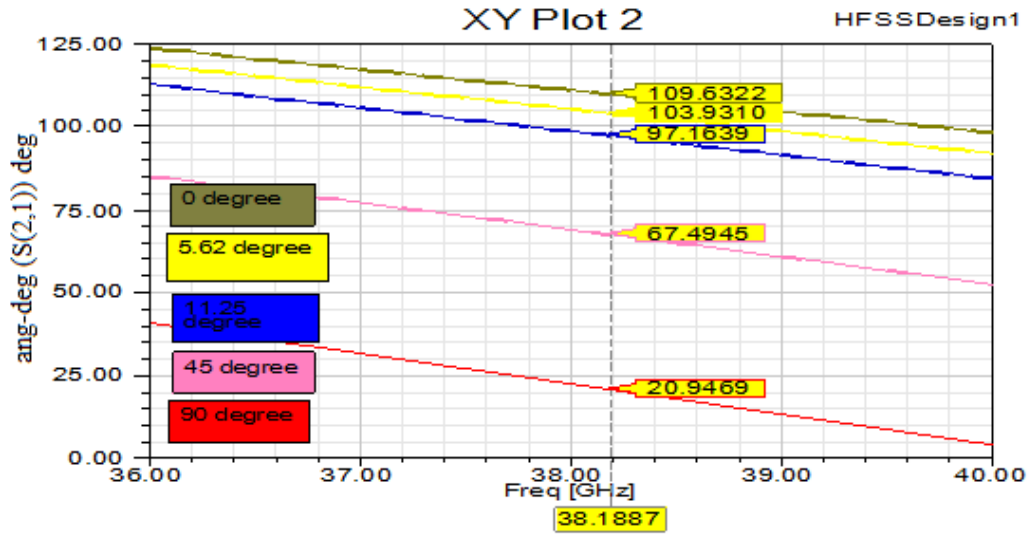

(a)

(b)

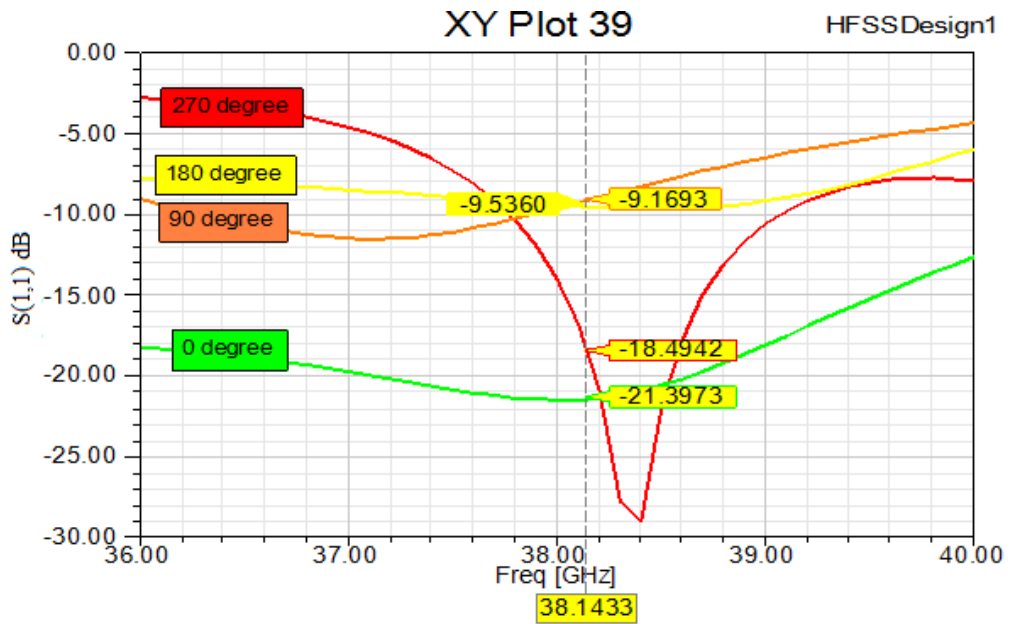Fig. 11. Simulation results of (a) phase and (b) return loss of the capacitor type section

it is seen, for all phases the return loss is less than -10dB. Fig. 13 shows the simulation results of the whole structure of the phase shifter.

Fig. 13a shows 90°, $(5.625+90)^o$ and $(16.875+90)^o$ phases with minimum errors. From the figures, the maximum error phase is around two degrees. Fig. 13b shows the corresponding return loss of the simulated phases. As it is seen, for all phases the return loss is less than -10dB.

Fig. 14 shows comparing obtained results by Matlab with HFSS simulation of the capacitor type section in 0°, -90° and11.25°
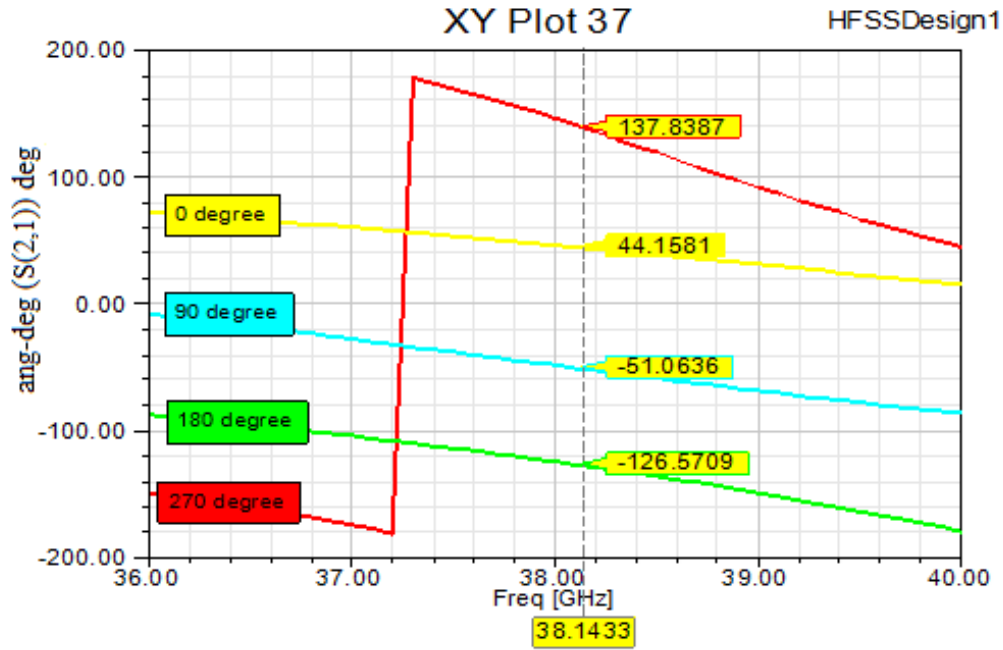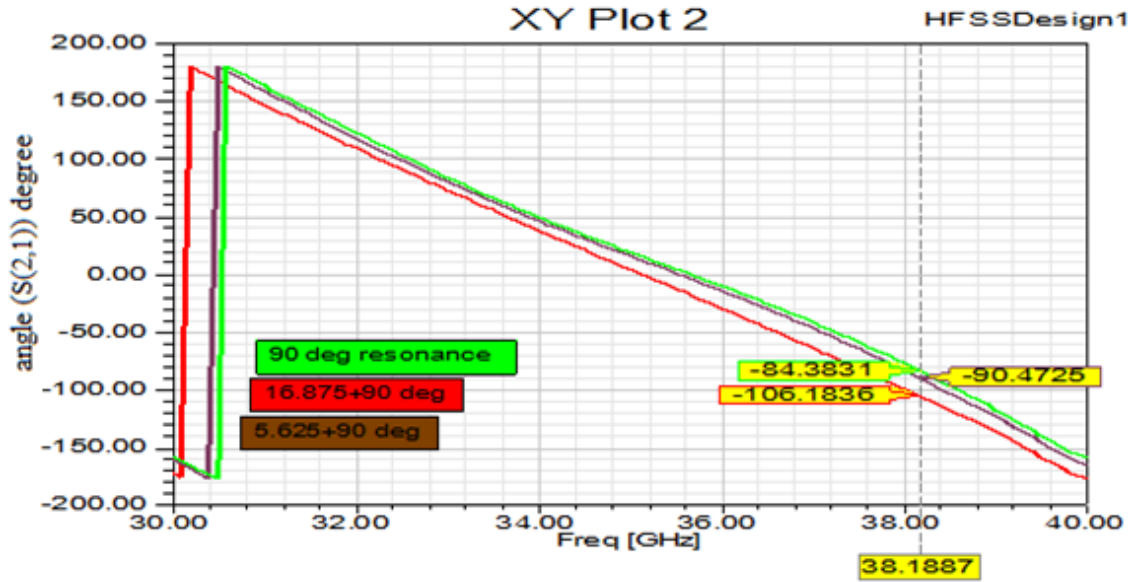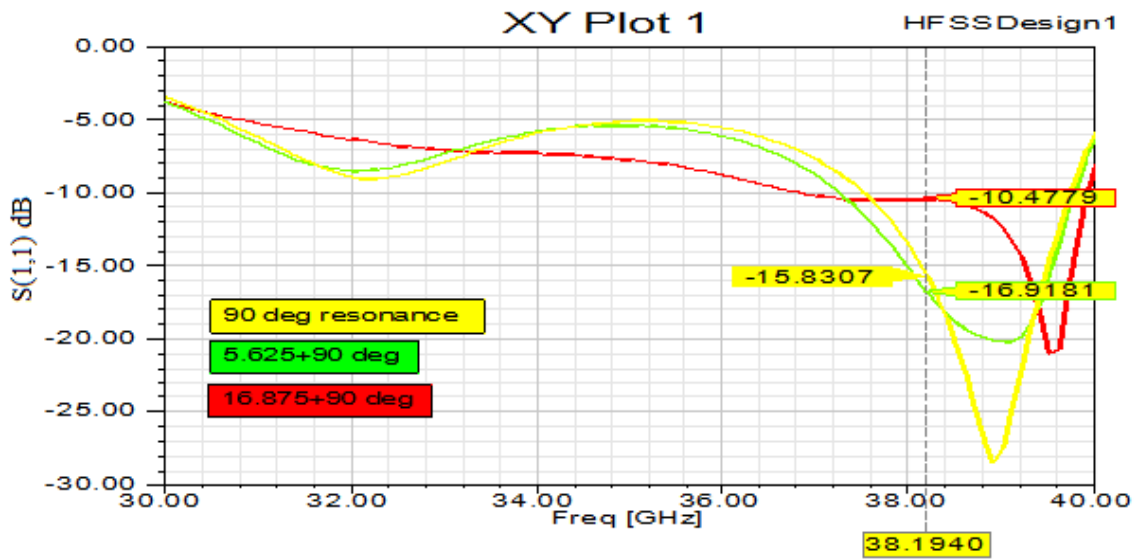

(a)

(b)

Fig. 12. Simulation results of (a) phase and (b) return loss of the resonator type section

Fig. 15 shows comparing obtained results by Matlab with HFSS simulation of the resonator type section in 0°, -90° and 270°.
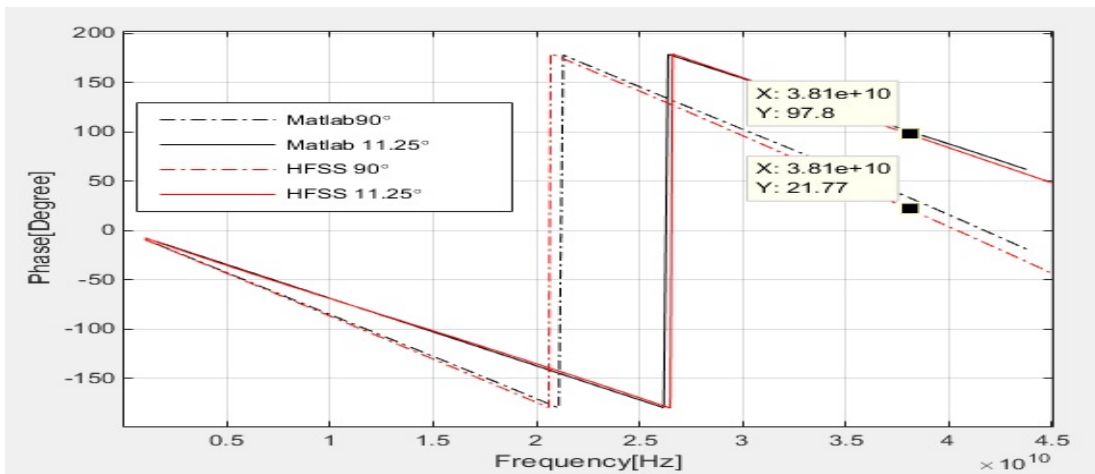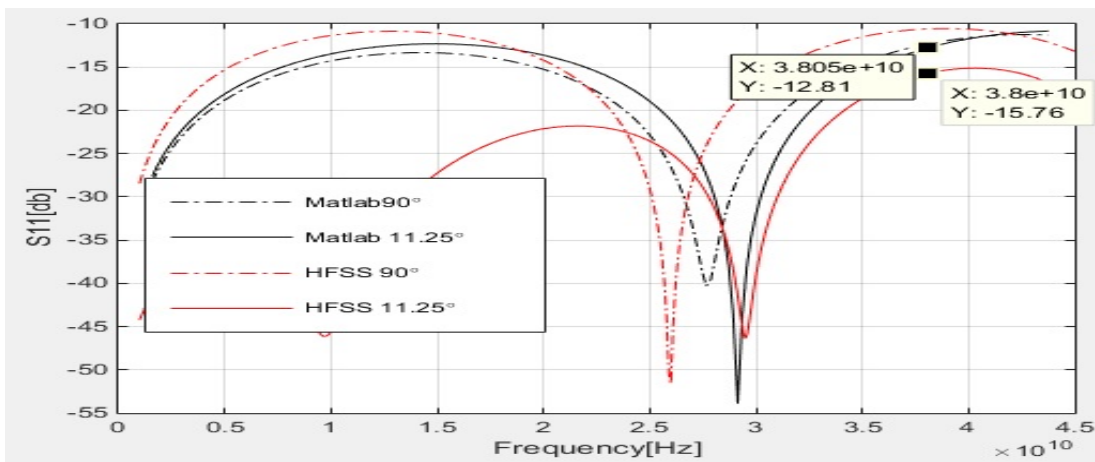

(a)

(b)

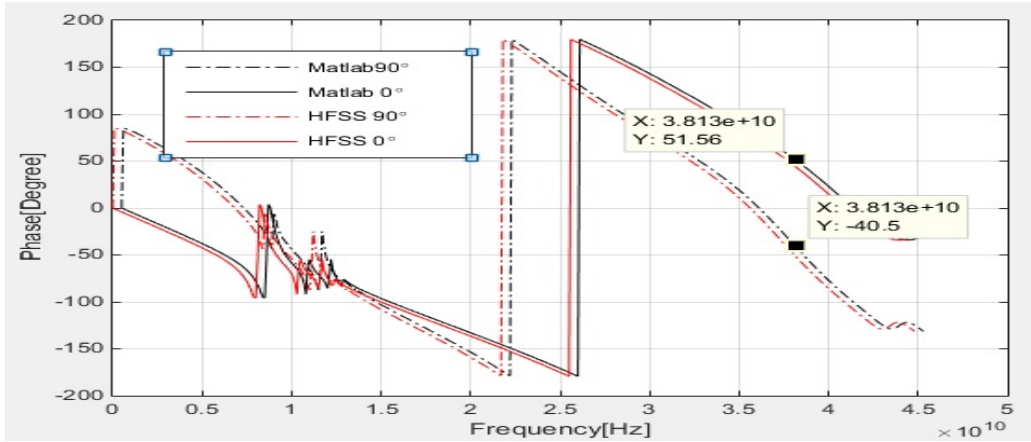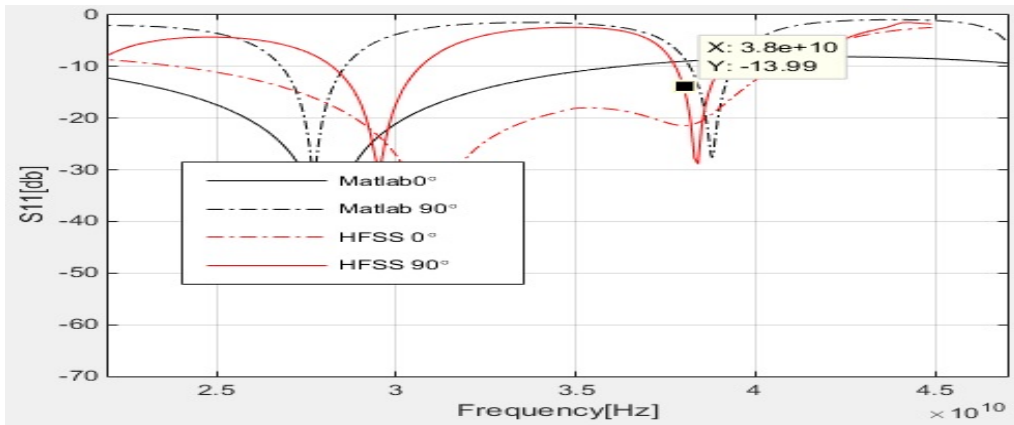Fig. 13. Simulation of results (a) phase and (b) return loss of the whole structure

(a)

(b)

Fig. 14. comparing obtained results by Matlab with HFSS simulation (a) phase and (b) return loss of
the capacitor type section

Fig. 16 shows comparing obtained results by Matlab with HFSS simulation of the whole structure in 90°
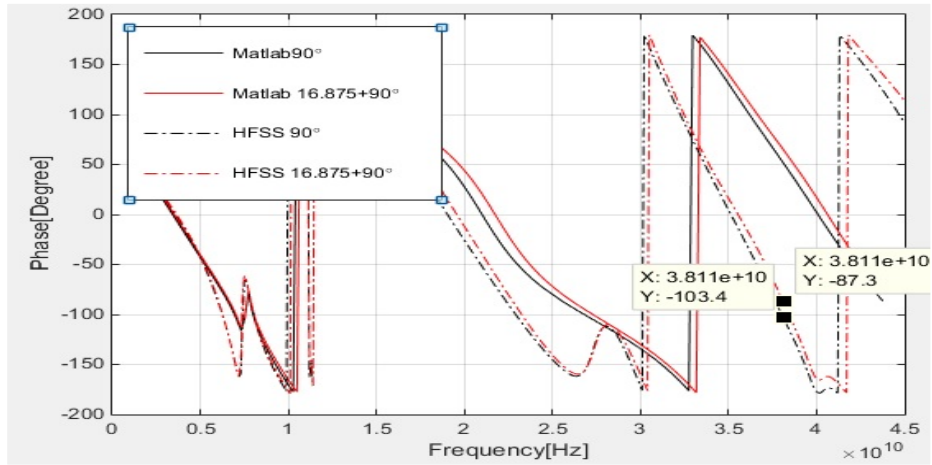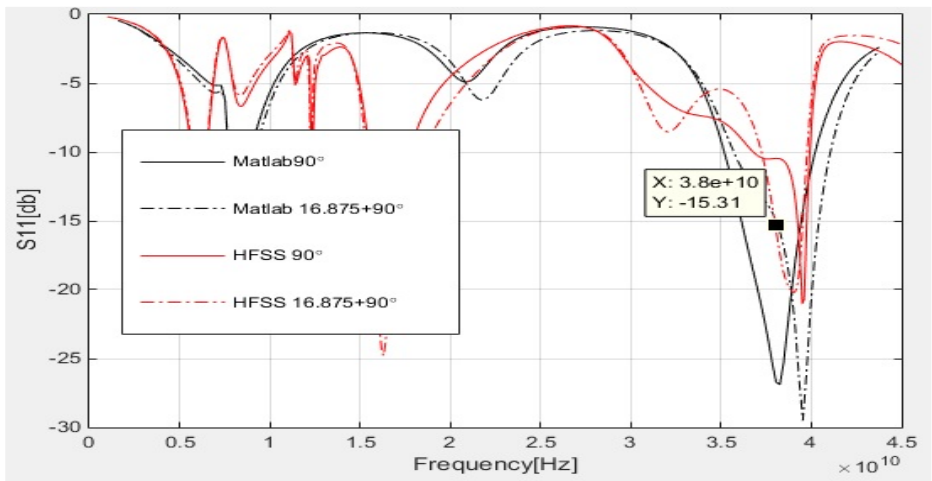and 90° +5.625°.

(a)

(b)

Fig. 15. comparing obtained results by Matlab with HFSS simulation (a) phase and (b) return loss of the
resonator type section

Table I shows the DMTL phase shifter performance comparison with the previously published phase
shifters.

(a)

(b)

Fig. 16. comparing obtained results by Matlab with HFSS simulation (a) phase and (b) return loss of the whole structure

Table I. Comparison of current state of the art DMTL phase shifters

Parameter	Afrang S [8]	Hayden J [5]	Liu Y [12]	This work
Frequency (GHz)	30	37.7	26	38.1
Bit number	6	2	3	6
Cell number	32	21	14	14
Total Length (mm)	12.8	8.4	11	6
Loss average	-0.6	-1.5	-1.7	-1.6
Max (return loss)	-11	-11.5	-7	-10
Max (phase error)	$2.1\,^\circ$	$1\,^\circ$	$8.5\,^\circ$	$1\,^\circ$
Unit cell length(μ)	400	400	780	400

IV. FABRICATION PROCESS

The proposed MEMS phase shifter is implemented on high resistivity silicon substrate. The CPW lines, the lower plates of MAM capacitors, MAM capacitor anchors, the lower plate of bridges and bias electrode plates are defined using a lift-off process by sputtering of Au layer. Next step is to increase the height of bias electrode plates, anchors and CPW line. It is done by defining and then electroplating of the mentioned area. In the third step, only the height of anchors is increased. Again, it is done by defining and then electroplating of the mentioned area. The forth step is to deposit and then define the dielectric layer on the bias electrode plates and lower electrode of the switches. To create the gap under the bridge it is needed to deposit and then pattern photoresist as a sacrificial layer. On the other hand the bridge will be rough due to the bias electrode plates. Therefore, before creating the sacrificial layer, to planarize the bridge, another photoresist is deposited and patterned. A 300/1000/1000-^{o}A Cr/Au/Ti seed layer is evaporated, and then patterned so that the bridges, excluding the area underneath and near the bridge, can be electroplated with Au at the same time.

To remove the sacrificial layer two methods can be used. These methods are dry and wet etching. In the dry etching, isotropic plasma etching is used. Wet etching is done using acetone. In wet etching method, to avoid collapsing the bridge during drying, the structure can be released using a critical point drying system. Finally, bonding wire as an inductor in the resonator type section is done using wire bonder equipment. The fabrication process of the proposed structure is similar to standard MEMS phase shifters. All facilities related to the fabrication of proposed DMTL phase shifter exist in Urmia MEMS lab.

V. CONCLUSION

A very small size 6-bit DMTL phase shifter was presented. It was done by a combination of the capacitor and resonator type phase shifters. Less and more significant bits were created by capacitor and resonator sections, respectively. The length of the proposed structure is 6mm. This is two times smaller than other 6-bit phase shifters in the literature. Due to decrease in size the total loss of the structure was decreased. The total phase errors are less than one and return loss for all states is smaller than -10dB. The structure was calculated at the Ka-band using MATLAB software. To verify, the structure was simulated by HFSS software.

REFERENCES

[1] C. F. Campbell and S. A. Brown, "A compact 5-bit phase-shifter MMIC for K-band satellite communication systems," *IEEE Trans. Microwave Theory Tech.*, vol. 48, no. 12, pp. 2652-2656, April 2000.

[2] K. Maruhashi, H. Mizutani, and K. Ohata, "A Ka-band 4-bit monolithic phase shifter using unresonated FET switches," *IEEE MTT-S Int. Microwave Symposium. Digest*, 51–54, June 1998.

[3] D. Uttamchandani, Handbook of MEMS for Wireless and Mobile Applications. Cambridge, U.K.: Woodhead, pp. 136–175, August 2013.

[4] N. S. Barker, and G. M. Rebeiz, "Distributed MEMS true-time delay phase shifters and wide-band switches," *IEEE Trans. Microwave Theory Tech*, vol. 46, no.11, pp. 1881-1890, November 1998.

[5] J. S. Hayden and G. M. Rebeiz, "Very low-loss distributed X band and Ka-band MEMS phase shifters using metal-air-metal capacitors," *IEEE Trans Microwave Theory Tech*, vol. 51, no. 1, pp. 309-314, January 2003.

[6] J-J Hung, L. Dussopt and G. M, Rebeiz, "Distributed 2- and 3-bit W-band MEMS phase shifters on glass substrates," *IEEE Trans Microwave Theory Tech*, vol. 52, no. 2, pp. 600-606, February 2004.

[7] S. Afrang, "Small size and low loss resonator type DMTL phase shifter," *Microelectronics Journal*, vol.44, no.5, pp. 442-453, May 2013.

[8] S. Afrang, K. Samandari and G. Rezazadeh, "A small size Ka band six-bit DMTL phase shifter using new design of MEMS switch," *Microsystem Technologies*, vol. 23, no. 6, pp. 1853-1866, June 2017.

[9] S. Afrang and B. Yeop Majlis, "Distributed transmission line phase shifter using MEMS switches and inductors," *Microsystem Technologies*, vol. 14, no. 8, pp. 1173-1183, August 2008.

[10] F. Lin, M. Wang, and M. RaisZadeh, "A Miniature Distributed Ku-Band Phase Shifter Using Tunable Inductors and MEMS Varactors," *National Wireless Research Collaboration Symposium*, 11-14, May 2014.

[11] H. M. Greenhouse, "Design of planar rectangular microelectronic inductors," *IEEE Trans. Parts, Hybrids, and Packaging,* vol. 10, no. 2, pp. 101-109, June 1974.

[12] Y. Liu, A. Borgioli, A. Nagra, and R. A. York, "K-band 3-bit low-loss distributed MEMS phase shifter," *IEEE Microwave Guided Wave Letter*, vol. 10, no. 10, pp. 415-417, October 2000.